TESTING OF A DELTA IV PAYLOAD ATTACH FITTING (PAF) SUBSTRUCTURE WITH AN INTEGRAL COMPOSITE FLANGE

John E. Higgins
Air Force Research Laboratory, VSSV
Kirtland AFB, NM USA

Greg Sanford
CSA Engineering, Inc.
Kirtland AFB, NM USA

Jeffry S. Welsh
Air Force Research Laboratory, VSSV
Kirtland AFB, NM USA

ABSTRACT

The Air Force Research Laboratory, Space Vehicles Directorate (AFRL/VS), has developed a unique composite Payload Attach Fitting (PAF) shell design. Alliant Techsystems (ATK) and the Boeing Company, Huntington Beach, CA, have developed manufacturing processes and a shell design that incorporates an all-composite forward flange with transverse reinforcement (Z-pinning) at key locations to prevent transverse separation and failure under high bending loads. This paper describes testing equipment, instrumentation, and procedures developed and executed by the AFRL in Albuquerque, NM to demonstrate the structural adequacy of the composite joint under increasing quasi-static load cycles near predicted failure. The overwhelmingly positive results obtained from this design and test program have led to new initiatives to develop modified designs for similar PAF structures.

BACKGROUND

The Delta IV PAF is a composite, conical shell residing between the payload and the upper launch vehicle interface. The primary function of the PAF is to taper the larger launch vehicle diameter to the smaller payload interface while providing adequate structural stiffness. For roughly a decade, typical composite PAF structures have been produced by hand lay-up of prepreg cloth material. Representative construction for this conic structure type uses a sandwich design with composite plies thinning at mid-height of the cone. Connecting flanges at the PAF forward and aft ends traditionally consist of thick, pre-fabricated aluminum inserts that are bonded and bolted to the composite shell. For the design described in the subject test program, the basic manufacturing process was converted to computerized placement of prepreg tow. The primary benefits of this conversion are to reduce the touch labor of hand-placed cloth and to reduce composite material waste by up to 40 percent (since wedge shapes need not be cut from linear bolts of cloth). Additional reductions in labor can be achieved by replacement of the metallic flange by simply continuing the placement of tow around the composite tool flange location. For the composite flange to resist interlaminar strains ATK reinforced limited regions at the bend of the flange with manually placed Z-pins. The flange fabrication process still requires precision drilling of bolted connection holes and final machining of the flange contact surfaces, but many other fabrication steps are avoided by eliminating the aluminum flange insert.

This paper will focus on experiment configuration, instrumentation, test procedures, and test facilities at the AFRL used to statically load a subcomponent of the full conic PAF. Instrumentation requirements were developed to monitor critically strained areas, to confirm uniformity of loading and response, and to assess the rotational stiffness of the all-composite flange. Cyclic testing in axial tension and compression were increased progressively to peak overload conditions of 175% of the design load for the PAF structure.

EXPERIMENT OBJECTIVES

The Boeing design team provided design requirements for this PAF including static test loads. Boeing developed the envelope of external loads for the

Report Documentation Page

Form Approved
OMB No. 0704-0188

1. REPORT DATE	2. REPORT TYPE	3. DATES COVERED
2004		**00-00-2004 to 00-00-2004**

4. TITLE AND SUBTITLE	5a. CONTRACT NUMBER
Testing of a Delta IV Payload Attach Fitting (PAF) Substructure with an Integral Composite Flange	5b. GRANT NUMBER
	5c. PROGRAM ELEMENT NUMBER
6. AUTHOR(S)	5d. PROJECT NUMBER
	5e. TASK NUMBER
	5f. WORK UNIT NUMBER
7. PERFORMING ORGANIZATION NAME(S) AND ADDRESS(ES) **Air Force Research Laboratory,ATTN: AFRL/VSSV,Kirtland AFB,NM,87117**	8. PERFORMING ORGANIZATION REPORT NUMBER
9. SPONSORING/MONITORING AGENCY NAME(S) AND ADDRESS(ES)	10. SPONSOR/MONITOR'S ACRONYM(S)
	11. SPONSOR/MONITOR'S REPORT NUMBER(S)

12. DISTRIBUTION/AVAILABILITY STATEMENT
Approved for public release; distribution unlimited

13. SUPPLEMENTARY NOTES
The original document contains color images.

14. ABSTRACT
see report

15. SUBJECT TERMS

16. SECURITY CLASSIFICATION OF:			17. LIMITATION OF ABSTRACT	18. NUMBER OF PAGES	19a. NAME OF RESPONSIBLE PERSON
a. REPORT	b. ABSTRACT	c. THIS PAGE			
unclassified	**unclassified**	**unclassified**		**8**	

PAF design from the launch vehicle and payload responses of heritage and predicted launch scenarios. The final PAF, designed to maintain stiffness and integrity under predicted launch loads, was designed as a fiber-placed, wound shell with an all-composite forward flange. The manufactured PAF is a full-scale test article with the exception of the overall height. Because the area of interest is primarily near the composite flange, the test article height was significantly shortened to approximately 596 mm (23.5 in). The forward composite flange has a bolt circle diameter of 178 cm (70.1 in) and an aft diameter of approximately 3050 mm (120 in). Both the full and modified test articles are shown in Figure 1 below.

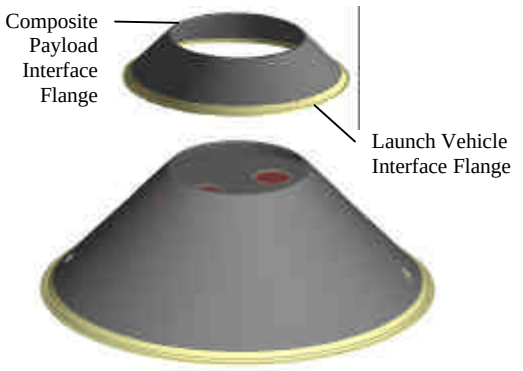

Figure 1. Full PAF and 360-degree test structure compared

The major objectives of this test series were as follows:

A. Observe and confirm that the composite flange could resist the repetitive and increasing loads well above the overall PAF design load without permanent distress or damage. Maximum applied tension and compression loading were limited to 175% of design since this value exceeds projected capacity of other portions of the PAF design.
B. Measure representative strain levels for the applied loads to confirm the nature of the structure response.
C. Measure overall structure displacement under the applied loads to confirm calculated structure stiffness.

Secondary objectives of this test series included the following:

A. Provide supplemental instrumentation to insure that intended loads and restraint conditions were met.
B. Measure rotation of the composite joint under tension and compression to confirm calculated flange rotational stiffness.

TEST CONFIGURATION

The 360-degree PAF substructure tests were conducted in a general-purpose steel frame load fixture commonly referred to as a reaction structure. The reaction structure in Figure 2 was used previously to flight qualify two payload adapter structures (EELV Secondary Payload Adapter (ESPA) for the EELV launch vehicle and a Multiple Payload Adapter (MPA) unit for the Minotaur launch vehicle). Because applied loads of earlier tests were well below the 2,224 kN (500,000 lbs) PAF axial load requirement, reaction structure stress and deflection magnitudes were analytically verified prior to the test. Displacement variation tolerances at the base of the test article, away from the composite flange, were required by Boeing to not exceed 0.76 mm (0.030 in). Both the frame peak stress and the displacements of the 13.3 cm (5.25 in) thick steel base plate were confirmed by analysis illustrated in Figure 3.

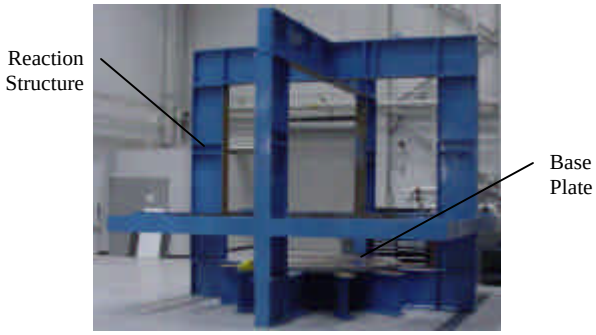

Figure 2. Reaction Structure with 13.3 cm thick circular base plate

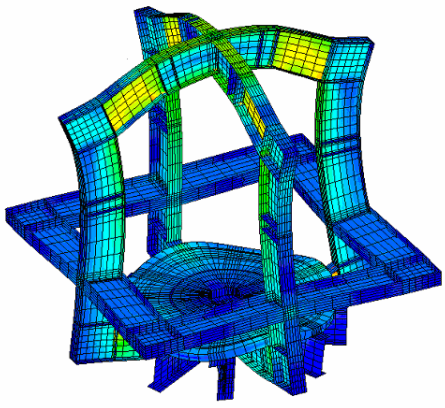

Figure 3. Example of reaction structure Von Mises stress distribution and displacement analysis

To suit the dimensions of the conic substructure a unique load head was fabricated to provide a sufficiently rigid test article interface. Five vertical actuators provided a distributed loading over the load

head: one actuator in the center of the load head and one on each cross beam, as shown in Figure 4.

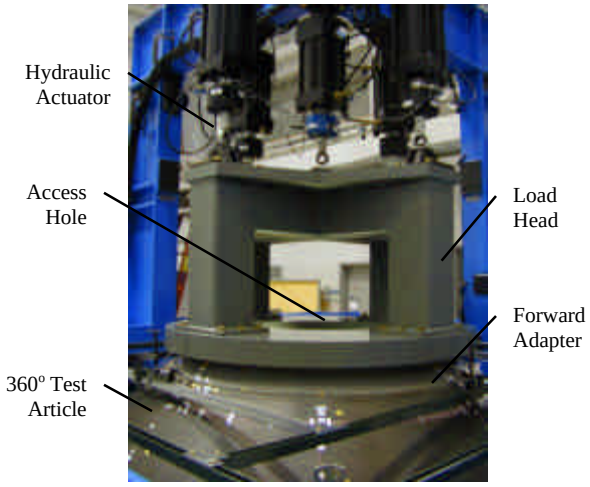

Figure 4. Load head and actuator assemblies

The base of the load head was a steel ring 10.8 cm (4.25 in) thick. This ring was designed to prevent unwanted load peaking by limiting local contact displacements with the aluminum forward adapter to less than 0.250 mm (0.010 in) (Figure 5). This ring also provided a serviceable personnel access to the interior of the test article where much of the instrumentation was located. Each actuator, rated for a maximum load of 445 kN (100,000 lbs), was positioned at the load frame and load head to within 2.5 mm (0.10 in) of the intended locations. Both actuator ends were connected via spherical rod end bearings pinned to a mounting clevis. In this configuration, the actuators were allowed three axes of rotational freedom at each end of the actuators to prevented actuator side loading.

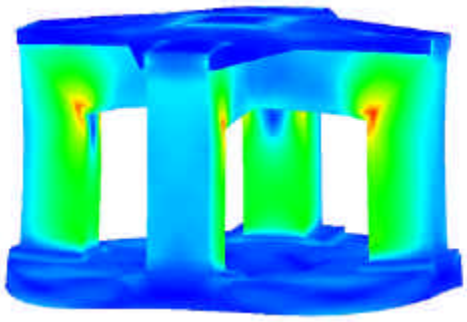

Figure 5. Example of load head Von Mises stress distribution and displacement analysis

Aluminum adapters were fabricated for attachment to the forward and aft ends of the test structure. Boeing designed and analyzed both adapters to approximate launch vehicle and payload compliance at each PAF interface. The aft adapter, representing the launch vehicle interface, consisted of a solid aluminum ring and four splice plates. Installation of the aft adapter onto the base plate is shown in Figure 6. Likewise, the forward adapter, representing the payload interface, was constructed of a solid aluminum ring as shown in Figure 7.

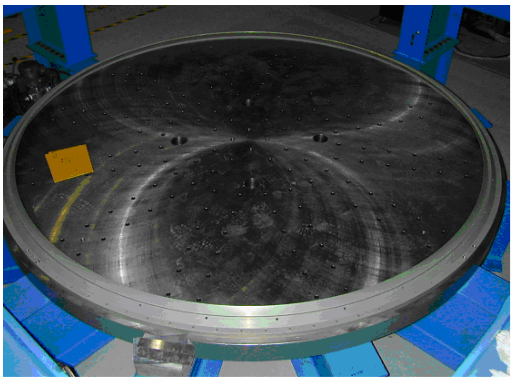

Figure 6. Aft adapter ring w/o splice plates (shown mounted to the reaction structure base plate)

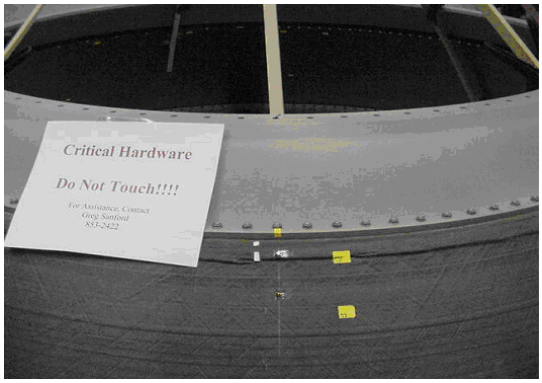

Figure 7. Forward adapter ring bolted to composite flange of test structure

INSTRUMENTATION

Instrumentation channels were conditioned, monitored, and recorded with a 256-channel Agilent® data acquisition system. The software interface, developed by MTS®, integrated and synchronized strain and displacement measurements with an Aero90 load controller. With this capability, both load cell bridges were recorded in concert with the instrumentation channels, thereby providing synchronized external load and response measurements. Additional software allowed the operator to monitor an unlimited number of channels during test operations while providing minimum and maximum limits used to suspend load application when reached. All channels, including load cells, were recorded at 1% increments of the flight load

while ramping up to the desired peak load for each cycle. When returning to zero load, however, data was recorded at 5% load increments. The fully populated data acquisition system is shown in Figure 8.

Figure 8. Populated Data Acquisition System

Strain Gages

A total of 42 uniaxial strain gages were monitored and recorded during testing (Figure 9). These strain gages were located to provide indications of critical strains in the region of the composite flange. Additional strain gages provided indications of uniform (axisymmetric) response in the overall test structure. Strain gage locations include uniaxial and biaxial gages placed on the inner and outer conic shell surfaces with a higher concentration near the forward composite flange. Typical strain gage locations shown in Figure 10 were installed at multiple azimuths around the shell.

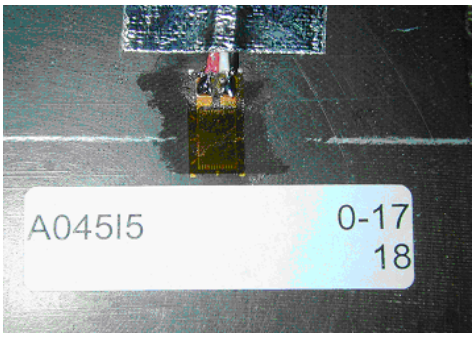

Figure. 9. Example of installed strain gage

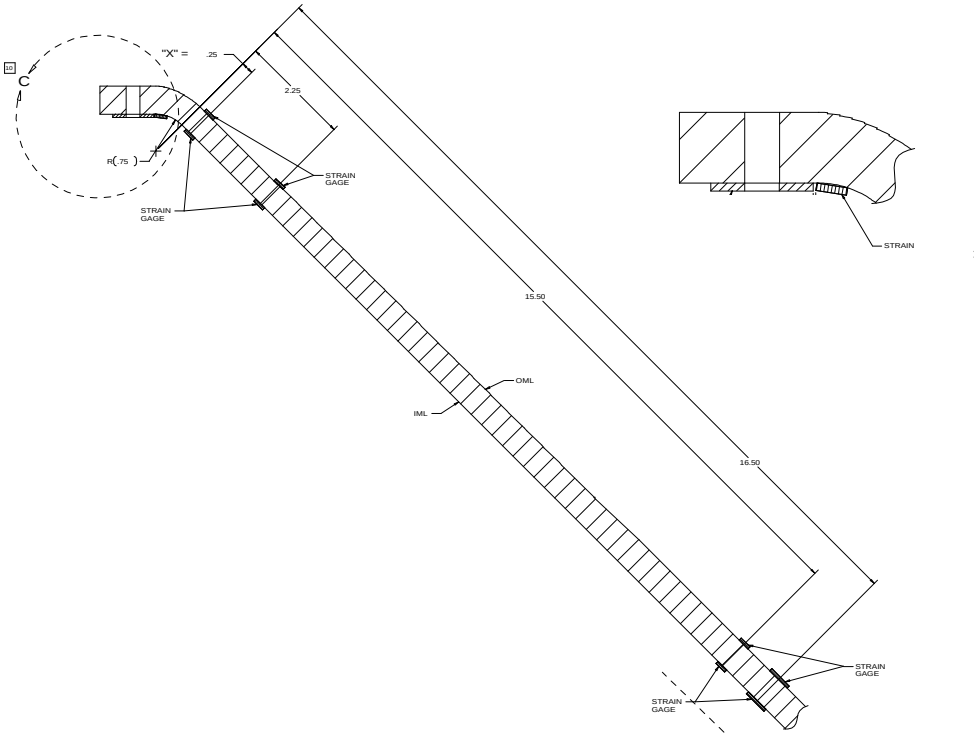

Figure. 10. Strain gage locations (view of conic shell cross-section)

Displacement Transducers

Displacement transducers were used at 14 locations to measure the overall axial displacement of the test article and the rotation of the forward flange. All transducers were attached to an isolated framework providing a reference to ground. Because of this configuration, all displacement measurements include reaction structure, base plate, and test article deflections. Six axial transducers near the aft PAF flange located at 45° intervals measured the deflection of the base plate and reaction structure. These measurements were used to normalize forward flange deflections, giving a clear reading of the overall test article deflection. Internal and external transducers at 90 degree intervals were used to measure rotation of the forward flange. Locations and orientation of both aft and forward flange displacements are shown in Figure 11.

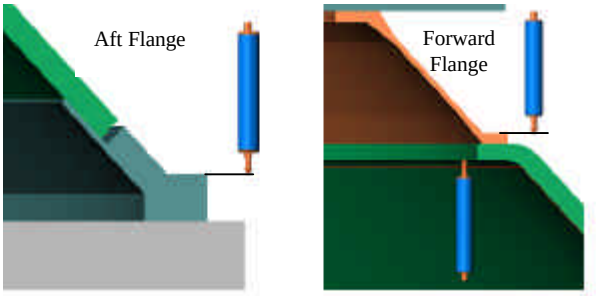

Figure 11. Displacement transducer locations

TEST OPERATIONS

The test series consisted of five load cases based on a percentage of flight loads in tension or compression. Load cases 1 and 2 required loading the test article to a nominal 40% (of flight load) followed by a 100% loading in tension (load case 1) and compression (load case 2). Similarly, load cases 3 and 4 required loading to 125% in tension and compression. The capability run, load case 5, completed the test series by alternating between tensile and compressive loads while gradually increasing load magnitudes until reaching 175%. A graphic representation of each load case is shown in Figure 12. Markers in the plot indicate hold points used for real-time data review during the test. Loads were uniformly increased at a rate of approximately 0.5% per second to simulate a static load scenario.

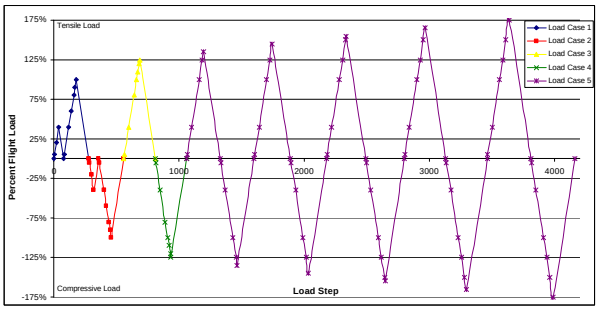

Figure 12. PAF load profile

The five actuators (labeled 000, 090, 180, 270, and Center in Figure 13) supplied all loads to the structure. Each load magnitude was divided equally among the five actuators with the exception of the Center actuator. The load on the Center actuator was different because it was used to off load gravity effects prior to testing. An initial bias of 31.1 kN (7,000 lbs) (upward) was applied to this actuator to account for the load head weight. Prior to the start of each test, the Center actuator bias was applied to counterbalance the load head weight, thereby simulating a zero load state on the test article. All strain gage and deflection transducers were subsequently zeroed and recorded as a baseline data record. This counterbalance operation was performed prior to the start of every load case. Load magnitudes for each actuator and total load applied to the test article are given in Table 1 for load case maxima. Corresponding to the data acquisition sampling rate, each 1% endpoint triggered the data acquisition recorder for load, strain gage, and displacement transducer records.

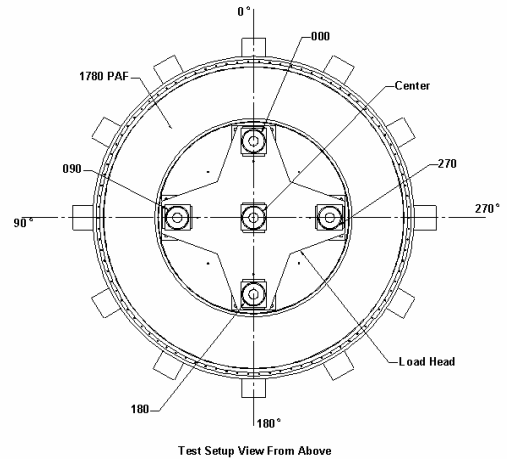

Figure 13. Actuator Reference Diagram

		Individual Actuator Loads					
		000	090	180	270	Center	Total Load*
Load Case	% Flight Load	N	N	N	N	N	N
1	40%	66617	66617	66617	66617	97754	357220
	100%	166541	166541	166541	166541	197679	856844
2	-40%	-85940	-85940	-85940	-85940	-54802	-405561
	-100%	-214849	-214849	-214849	-214849	-183712	-1050108
3	125%	208177	208177	208177	208177	239314	1065021
4	-125%	-268561	-268561	-268561	-268561	-237424	-1318669
5	135%	224831	224831	224831	224831	255968	1148292
	-135%	-290046	-290046	-290046	-290046	-258909	-1426094
	145%	241485	241485	241485	241485	272623	1231563
	-145%	-311531	-311531	-311531	-311531	-280394	-1533518
	155%	258139	258139	258139	258139	289277	1314833
	-155%	-333016	-333016	-333016	-333016	-301878	-1640943
	165%	274793	274793	274793	274793	305931	1398104
	-165%	-354501	-354501	-354501	-354501	-323363	-1748367
	175%	291447	291447	291447	291447	322585	1481375
	-175%	-375986	-375986	-375986	-375986	-344848	-1855792

*Includes wieght of load head

Table 1. Actuator loads for each load case

RESULTS

On day one, Load Case 1 was attempted and aborted at 1% load as a result of a communication error between the load control and data acquisition systems. An exhaustive system checkout revealed a damaged digital input/output (DIO) cable used to trigger data acquisition. Upon repair, the communication link was restored and test operations continued. No problems were reported during the initial 40% run. During the limit (100%) run, a large cracking noise was heard at approximately 43% load. While many strain and displacement sensors showed a significant shift, the load controller maintained load and the test continued to 100% without further incident. The entire load case was subsequently re-run in an attempt to obtain a more continuous data set. No noises or data shift were witnessed during the second attempt. Visual inspection of the test article showed no indication of damage.

Load Case 2 was also successfully completed on the second day of testing. No problems were reported during the initial 40% run. During the limit (100%) run, a loud bang was heard at ~45% load. Load in the structure was altered enough to cause a load controller-induced test abort. Inspection of the high-speed shutdown recorder gave no indication of a significant load spike, indicating a successful abort. No test article damage was found, so the entire load case was re-run. No anomalies or noises were noted during the second attempt; however, most instrumentation channels showed significant hysteresis while unloading. This 100% loading was applied a third time in an attempt to obtain a more continuous data set. This attempt proved successful, but a very minor cracking noise was noted just below 100% while returning to zero. Inspection of the test article showed no indication of damage.

Day two testing continued through the successful completion of both Load Case 3 and 4. With the exception of hysterises, no problems were noted during the first 125% run. The load case was re-run to obtain a smoother data set. This test was re-run successfully and no test article damage was noted. During Load Case 4, minor cracking noises were noted at 109%, 122%, and 124% while ramping up to 125%. The load case was re-run to obtain a smoother data set. The test was re-run successfully and no test article damage noted.

On day three, Load case 5 was successfully completed. The four displacement transducers on the inside forward flange were biased prior to the start of the test because compressive deflections in this region were expected to be larger than the sensor range. Because of this bias, data during tensile tests quickly "flat-lined" as the transducers ran out of outward stroke. Data from the compressive loads, however, remained valid. All load cycles up to 175% were completed without incident. A minor cracking noise was heard at 138% of the compressive 145% run. Another minor noise was heard at 149% of the 155% compressive run. A strain gage limit was reached at 174% of the compressive 175% causing a system hold. The limit was deactivated, and the test was completed. Inspection of the test article showed no indication of damage.

Instrumentation Notes

Strain gages near the forward, composite flange were monitored throughout testing operations to help assess the uniformity of applied loads around the test article's circumference. Five such strain gages encompassing a 100° segment of the PAF are plotted in Figure 14. The representative gages were located on the inside shell surface, 6.35 mm (0.25 in) below the upper composite flange. Data represented here shows strain levels at 125% axial, tensile load (Load Case 3). As predicted, the maximum strain magnitude is found directly below an actuator attach point corresponding to the 90° location. The difference between the maximum and minimum strains in the region, 10%, is a useful estimate of the load peaking imparted into the structure. Load peaking of this magnitude is comparable to actual flight conditions, making it well within acceptable limits.

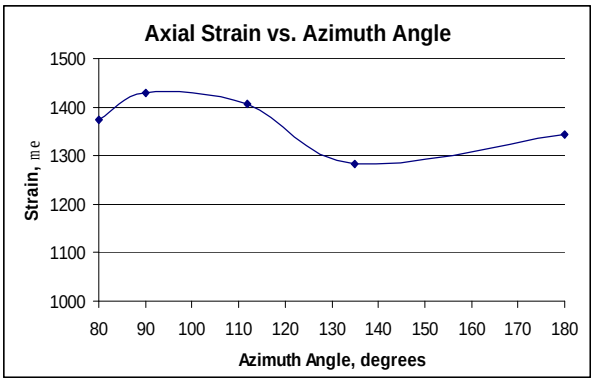

Figure 14. Representative load peaking plot

Significant hysteresis was noted for the first run of virtually all load cases. While hysteresis can be an indication of permanent deformation or yielding in the structure, this was not the case for these tests. As with most structures containing complex bolted joints, relatively small amount of joint slippage can significantly alter load paths, causing non-linear strain and deformation readings. A linear response is found while loads return to zero, creating linear unloading curves. This behavior is seen in every load case because loads alternate from tension to compression as previously shown in Figure 12. For example, upon completion of Load Case 1, the bolted joints have slipped due to the tension load. Applying the compressive load of Load Case 2 slips the joint in the opposite direction, and so on for each subsequent loading scenario.

As mentioned in the results of the individual load cases, the tests were re-run to obtain a smoother, less-hysteretic data set. Both the first and second runs of Load Case 4 illustrate this behavior for a typical upper flange, axial strain gage in Figure 15. Non-linear strain response is clearly visible as the load path is altered during loading, followed by a linear unloading curve. Once the joint has been "set" from the compressive load, a clean loading and unloading curve is shown for the second run of identical loading. While these slips are the result of very small deflections, they further illustrate the benefits of reducing complex bolted joints with continuous designs such as the integrated composite PAF flange.

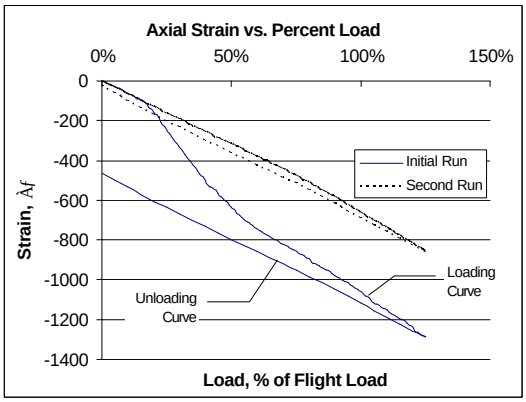

Figure 15. Example of hysteresis

One of the additional test objectives was to quantify the forward, composite flange rotation under tensile and compressive loads. An accurate rotation estimate is a critical data record used to compare to metallic-flange PAF structures. Analytical estimates of this region show sufficient rotational stiffness, an assumption that can only be verified through actual test data.

As described in the Displacement Transducer section and shown in Figure 11, four sets of displacement transducers were used to assess this rotation. Assuming the flange rotates as a rigid body about the theoretical hinge defined as the intersection of the mid-planes of the conic shell and flange, the rotation was estimated by post-processing the acquired data. Data shown in Figure 16, shows calculated flange rotations at the four transducer locations for each maximum loading condition. Maximum flange rotation at 175% load was found to be 3.3°.

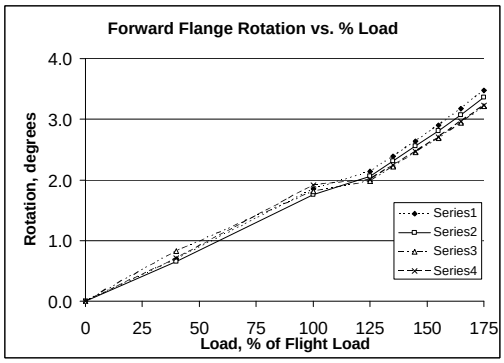

Figure 16. Rotation of forward (composite) flange

CONCLUSIONS

The only significant events (a loud bang) occurred during the early stages of Load Cases 1 and 2 (43% and 45% respectively). This behavior did not continue at higher loads, indicating a shift in the structure due to an initial constrained condition. Though not pinpointed by acoustic measurements, the most probable cause was bolt slippage in the splice joint of the aft adapter ring. Here, a layer of steel-filled epoxy was applied to fill gaps between the composite shell and the rolled splice plates. Acting as a brittle adhesive, the epoxy may have locally disbonded, thereby transferring load to the many bolts in the region. Once these bolts began to carry loads in shear, the structure could shift when reversing the load from tension to compression as a result of slightly oversized holes. This type of event commonly causes hysteresis.

All loading operations were successfully performed with each load applied within a predetermined tolerance (±0.3%) at each data record. Strain, deflection, and load data were successfully recorded for all load cases. The all-composite flange carried 175% of the predicted axial launch loads in both tension and compression, thereby meeting the major test objectives.

REFERENCES

1. Sanford, G.E., "Development and Structural Qualification of the EELV Secondary Payload Adapter (ESPA)", 43rd AIAA/ASME/ASCE/ AHS/ASC Structures, Structural Dynamics, and Materials Conference, Paper No. 1698, Denver, CO, April 2002.

2. Sanford, G.E. and Welsh, J.S., "Static Testing of the EELV Secondary Payload Adapter (ESPA)", SEM Annual Conference on Experimental and Applied Mechanics, Paper No. 83, Charlotte, NC, June, 2003.

3. Higgins, J.E., Sanford, G.E., and Welsh, J.S., "Advanced Iso-Grid Fairing Qualification Test for Minotaur Launch Vehicle", 14th International Conference on Composite Materials, Paper No. 752, San Diego, CA, July, 2003.